Heat balance analysis for self-heating torrefaction of dairy manure using a mathematical model

Takanori Itoh [a,b], Teppei Ogawa [c], Kazunori Iwabuchi [b,*], Katsumori Taniguro [a]

[a] Tanigurogumi Corporation, Shiobara 1100, Nasushiobara, Tochigi 329-2921, Japan

[b] Research Faculty of Agriculture, Hokkaido University, Kita 9, Nishi 9, Kita-ku, Sapporo, Hokkaido 060-8589, Japan

[c] Graduate School of Agriculture, Hokkaido University, Kita 9, Nishi 9, Kita-ku, Sapporo, Hokkaido 060-8589, Japan

*Corresponding author: iwabuchi@agr.hokudai.ac.jp (K.I.)

Abstract

A self-heating torrefaction system was developed to overcome the difficulties in converting high-moisture biomass to biochar. In self-heating torrefaction, the ventilation rate and ambient pressure must be set properly to initiate the process. However, the minimum temperature at which self-heating begins is unclear because the effects of these operating variables on the heat balance are not theoretically understood. The present report presents a mathematical model for the self-heating of dairy manure based on the heat balance equation. The first step was to estimate the heat source; experimental data showed that the activation energy for the chemical oxidation of dairy manure is 67.5 kJ/mol. Next, the heat balance of feedstock in the process was analyzed. Results revealed that the higher the ambient pressure and the lower the ventilation rate at any given pressure, the lower the temperature at which self-heating is induced. The lowest induction temperature was 71 °C at a ventilation rate of 0.05 L min^{-1} kg-AFS^{-1} (AFS: ash-free solid). The model also revealed that the ventilation rate significantly affects the heat balance of feedstock and drying rate, suggesting an optimal range for ventilation.

Keywords

Biochar; Drying; Pyrolysis; Self-heating; Torrefaction; Torrefied biomass

1. Introduction

While the application of manure-derived fertilizers to fields is a basic strategy for establishing a carbon and fertilizer recycling system, the increase in manure generation associated with expansion of the livestock industry raises concerns about environmental problems such as water pollution (Basso and Ritchie, 2005; Maeda et al., 2003), and odors

and greenhouse gas emissions due to improper manure management (Amon et al., 2006). In addition, the risk of environmental contamination by antibiotics in manure has been recognized recently as an emerging issue (Muhammad et al., 2020; Spielmeyer, 2018). These factors have increased the importance of developing new livestock manure management techniques.

Thermochemical conversion of livestock manure is an alternative route for manure management because it alters the manure properties to make it suitable for use as a solid fuel and/or soil conditioner (Chen et al., 2021; Li and Jiang, 2017). Hydrothermal carbonization (also called wet torrefaction)—hydrothermally decomposing biomass in subcritical water (180–260 °C) for minutes to hours—appears to be the first option for livestock manure due to its high moisture content (He et al., 2018; Wang et al., 2018). Despite the great potential of hydrothermal carbonization, the necessity of post-process water treatment by chemical or biological means may prevent its implementation on a large scale (Wirth and Mumme, 2014; Wirth and Reza, 2016). To avoid this problem, a self-heating torrefaction system has been proposed that uses heat from the chemical oxidation of the feedstock as an energy source for drying and pyrolysis (Itoh et al., 2020, 2019). Self-heating torrefaction is similar to oxidative pyrolysis—which uses the heat source generated by partial combustion of the feedstock (Daouk et al., 2017; Milhé et al., 2013; Pham et al., 2018; Rizzo et al., 2019)—but differs significantly in that it should also accept high-moisture biomass that does not continue self-sustained combustion.

From a macroscopic view, the self-heating of biomass occurs when the amount of heat generated by biological and chemical oxidation exceeds the amount of heat loss due to

water evaporation and heat release from the biomass surface. Self-heating of manure, typified by composting, is a common phenomenon when a certain degree of insulation and oxygen supply is ensured. Meanwhile, self-heating that leads to self-ignition of biomass rarely occurs in nature, because, as temperatures increase, the amount of heat loss due to water evaporation also increases, while microbial activity decreases. To intentionally induce self-heating of manure that reaches 300 °C, the proposed torrefaction system provides a continuous oxygen supply under high pressure to promote chemical oxidation and greatly reduce water evaporation at around 100 °C. Thus, the torrefaction system requires the proper setting of operating variables such as ventilation rate (for oxygen supply) and ambient pressure to induce self-heating. Therefore, it is crucial to determine theoretically the minimum temperature at which the self-heating of livestock manure due to chemical oxidation can be induced. A previous study reported that at a pressure of 1.0 MPa and ventilation rate of 0.83 ± 0.02 L min^{-1} kg-AFS^{-1} (AFS: ash-free solid), self-heating of dairy manure due to chemical oxidation begins at 85–90 °C (Itoh et al., 2019). Another study found that higher temperatures are required to induce self-heating at lower ambient pressures (Itoh et al., 2020). Experimental studies to date have provided some understanding of the effect of pressure on the heat balance of the feedstock, but a full understanding of the effect of operating variables, including ventilation rate, is not yet available.

A mathematical model based on the heat balance equation could be useful to answer the above question. Some mathematical models have been proposed to describe the self-heating of biomass (Sheng and Yao, 2022), composting (Walling et al., 2020), and oxygen-lean torrefaction (Kung and Ghoniem, 2019). However, they assume a constant

atmospheric pressure (0.1 MPa), and no model takes into account variations in ambient pressure, which should affect heat loss due to water evaporation. Additionally, the accuracy of the models depends on the accuracy of the heat source estimates. Only activation energies for pyrolysis and combustion of manure have been reported (Fernandez-Lopez et al., 2016; López-González et al., 2017), whereas no data are available for that of low-temperature oxidation. The goal of the present study was to determine mathematically the effects of ambient pressure and ventilation rate on the heat balance of biomass during self-heating torrefaction. A simplified mathematical model was constructed to estimate the parameters related to the heat generation term from the experimental data, validate the reliability of the model, and investigate the effect of operating variables on the heat balance of biomass during the process.

2. Material and methods

2.1. Experiments

Experiments were conducted in a manner similar to studies published previously (Itoh et al., 2020, 2019). Briefly, a cylindrical stainless-steel reactor with 0.83×10^{-3} m^3 effective volume containing 200 g of wet dairy cattle manure with a moisture content of about 60% on a wet basis and an ash content of 15% on a dry basis was placed in an STPH-102M oven (Espec, Osaka, Japan). An air supply from the bottom of the reactor to the top was provided by an air cylinder and F-201CV series mass flow controller (Bronkhorst Japan, Tokyo, Japan). Ambient pressure inside the reactor was maintained at the desired pressure with a BP-3 series back-pressure regulator (Go Regulator, Spartanburg, SC, USA). To induce self-heating, the reactor was heated in an oven at a given inducing temperature. Once the sample temperature exceeded the preset oven temperature due to self-heating,

the oven temperature was controlled to within 1.5 °C of the sample temperature to improve thermal insulation.

2.2. Mathematical model

2.2.1. Governing equation

In this study, the mathematical model was simplified so it did not affect the quantification of the heat produced by biomass oxidation. This results in the following assumptions: (1) no decomposition of biomass occurs; (2) no gradient in oxygen concentration, temperature, or moisture content inside the biomass is present; (3) no heat loss occurs from the reactor wall to the surroundings; (4) gas temperature at the outlet is always equal to biomass temperature; and (5) the specific heat capacity of moist air, water, and biomass is constant. Based on these assumptions, a temperature change in the biomass is given by

$$(\theta_{\mathrm{S}}\rho_{\mathrm{S}}c_{\mathrm{S}} + \theta_{\mathrm{L}}\rho_{\mathrm{L}}c_{\mathrm{L}})\frac{\mathrm{d}T}{\mathrm{d}t} + \dot{m}_{\mathrm{G}}c_{\mathrm{G}}(T - T_{\mathrm{G}}) = Q_{\mathrm{Dry}} + Q_{\mathrm{Oxi}}, \quad (1)$$

where θ is the volume fraction (-), ρ is the density (kg/m^3), c is the specific heat capacity at constant pressure (kJ kg^{-1} K^{-1}), T is the biomass temperature (K), T_{G} is the inlet gas temperature (K), t is time (s), $\dot{m}_{\mathrm{G}}$ is the mass flow rate of dry air ($\dot{m}_{\mathrm{G}}$ [kg s^{-1} m^{-3}]), Q_{Dry} is the heat consumed for drying (kW/m^3), and Q_{Oxi} is the heat generated by oxidation (kW/m^3) (the subscripted S, L, and G represent dry biomass, water, and air, respectively).

The values of density and specific heat capacity of dry biomass (ρ_{S} and c_{S}) were estimated to be 1.53 × 10^3 kg/m^3 and 1.4 kJ kg^{-1} K^{-1}, respectively (Dupont et al., 2014; Iwabuchi et al., 1999). The specific heat capacity of wet air (c_{G}) was calculated to be ≈1.00 kJ kg^{-1} K^{-1} with the specific humidity of inlet gas of 0.0017 $\mathrm{kg_{vapor}/kg_{dry\ air}}$. From

133 the experimental setup (0.08 kg of dry biomass and 0.12 kg of water packed in a reactor
134 with an effective volume of 0.83×10^{-3} m^3) and densities, the volume fraction of solid
135 (θ_S) was 0.063 and the initial volumetric water content ($\theta_{L,0}$) was 0.146.
136
137 *2.2.2. Drying*
138 The heat loss from drying [Q_{Dry} (kW/m^3)] was expressed as the product of the latent heat
139 of water evaporation ($h_v = \{2{,}500 - 2.44(T - 273.15)\}$ [kJ/kg]) and the drying rate
140 ($R_{Dry} = \rho_L(-d\theta_L/dt)$ [kg s^{-1} m^{-3}]),

141 $$Q_{Dry} = -R_{Dry} h_v. \quad (2)$$

142 Since drying occurs with the difference in specific humidity as the drying force, the drying
143 rate was expressed using the characteristic function for drying $f(\theta_L)$ (Toei et al., 1994):

144 $$R_{Dry} = \rho_L \left(-\frac{d\theta_L}{dt}\right) = f(\theta_L)\dot{m}_G(H_T^* - H_G), \quad (3)$$

145 where H_T^* is the supposed saturated humidity at the supposed biomass temperature of T
146 ($kg_{vapor}/kg_{dry\ air}$) and H_G is the specific humidity of gas ($kg_{vapor}/kg_{dry\ air}$).
147
148 The characteristic function for drying, $f(\theta_L)$, changes its form based on the stage of
149 drying, with $f(\theta_L) = 0$ for the preheating period and $f(\theta_L) = 1$ for the constant rate of
150 the drying period. During the decreased rate of the drying period, the function becomes
151 one of moisture content. The form of the expression depends on the shape of the biomass
152 and the state of water retention. The assumptions here are as follows: (1) the decreased
153 rate drying curve is proportional to the moisture content, (2) the equilibrium moisture
154 content ($\theta_{L,e}$) is nearly 0 because the biomass is heated to the torrefaction temperature
155 after drying, and (3) the critical moisture content ($\theta_{L,c}$) is nearly equal to the initial

moisture content ($\theta_{\mathrm{L},0}$) according to a previous report (Tojo et al., 1994). With these assumptions, the drying characteristic function is expressed as

$$\mathrm{f}(\theta_{\mathrm{L}}) = \frac{\theta_{\mathrm{L}} - \theta_{\mathrm{L,e}}}{\theta_{\mathrm{L,c}} - \theta_{\mathrm{L,e}}} \approx \frac{\theta_{\mathrm{L}}}{\theta_{\mathrm{L},0}}. \quad (4)$$

Then, the drying rate is given by

$$R_{\mathrm{dry}} \approx \frac{\theta_{\mathrm{L}}}{\theta_{\mathrm{L},0}} \dot{m}_{\mathrm{G}} (H_T^* - H_{\mathrm{G}}). \quad (5)$$

The saturated humidity can be obtained using total pressure (p_{total} [Pa]) and saturation vapor pressure ($p_{\mathrm{s}}(T)$ [Pa]):

$$H_T^* = \frac{M_{\mathrm{v}}}{M_{\mathrm{air}}} \frac{p_{\mathrm{s}}(T)}{p_{\mathrm{total}} - p_{\mathrm{s}}(T)}, \quad (6)$$

where M_{v} and M_{air} are molar mass of water vapor (18×10^{-3} kg/mol) and molar mass dry air (29×10^{-3} kg/mol), respectively. Saturation vapor pressure, a function of temperature, was computed using the Wagner equation (Wagner and Pruss, 1993).

2.2.3. Oxidation

Chemical oxidation generates heat that induces self-heating of biomass. The reaction produces not only carbon dioxide and water, but also a small amount of carbon monoxide and hydrocarbons. Although predicting the amount of each component in detail might be possible, obtaining the overall energy balance was the goal rather than predicting the precise amount of each component. A previous study found that the oxygen consumption rate increased with temperature and eventually equaled the oxygen supply rate at temperatures above 140 °C (Itoh et al., 2019), indicating that the equation describing the oxidation reaction must be divided according to the relation between oxygen consumption and supply rates. Thus, the rate of chemical oxidation was assumed to follow the

Arrhenius equation while the oxygen consumption rate ($v_{\mathrm{O_2,CONS}}$ [mol m^{-3} s^{-1}]) was smaller than the oxygen supply rate ($v_{\mathrm{O_2,SPLY}}$ [mol m^{-3} s^{-1}]) and depended on the oxygen supply rate when the consumption and supply rates were approximately the same:

$$Q_{\mathrm{oxi}} = \begin{cases} \theta_{\mathrm{S}}\rho_{\mathrm{S}}Q_{\mathrm{b}}A\exp\left(-\dfrac{E_{\mathrm{a}}}{RT}\right) & v_{\mathrm{O_2,CONS}} < v_{\mathrm{O_2,SPLY}}, \\ -\Delta H_{\mathrm{CO_2}}\dfrac{x_{\mathrm{O_2}}}{M_{\mathrm{air}}}\dot{m}_{\mathrm{g}} & v_{\mathrm{O_2,CONS}} \approx v_{\mathrm{O_2,SPLY}}, \end{cases} \quad (7)$$

where Q_{b} is the heat of reaction (kJ/kg), A is a pre-exponential factor (1/s), E_{a} is apparent activation energy (kJ/mol), R is a gas constant (J K^{-1} mol^{-1}), $\Delta H_{\mathrm{CO_2}}$ is the standard enthalpy of formation of carbon dioxide (−394 kJ/mol), and $x_{\mathrm{O_2}}$ is the mole fraction of oxygen (0.21 mol/mol$_{\mathrm{air}}$). For simplification, the following assumptions were made: (1) enough biomass is present compared to supplied oxygen ($[\mathrm{O_2}] \ll [\mathrm{Biomass}]$), and (2) the formation of carbon dioxide is the sole heat source. To determine the activation energy and pre-exponential term of $\theta_{\mathrm{S}}\rho_{\mathrm{S}}Q_{\mathrm{b}}A$, the Arrhenius plot was determined using the temperature data obtained in a previous study (Itoh et al., 2019).

3. Results and discussion

3.1. Estimate of heat source

Figure 1a shows the Arrhenius plot created using the experimental data. The plot was highly linear from 112 to 126 °C (0.00260 to 0.00251 [1/K]) but lost linearity over the rest of the temperature range. Estimating the Arrhenius parameters using the temperature range with the greatest linearity (R^2 = 0.969), the activation energy (E_{a}) and pre-exponential term ($\theta_{\mathrm{S}}\rho_{\mathrm{S}}Q_{\mathrm{b}}A$) of manure for chemical oxidation were 67.5 kJ/mol and 1.27×10^9 kW/m^3, respectively (Fig. 1b).

Sheng and Yao (2022) summarized that the activation energy of various types of lignocellulosic biomass for chemical oxidation ranged from 72 to 136 kJ/mol, with an average of *ca*. 90 kJ/mol. The presence of carbohydrates and other readily degradable organic matter in dairy cattle manure makes it reasonable that the activation energy of dairy cattle manure is lower than that of such biomass. The loss of linearity at temperatures higher than 130 °C (<0.00248 [1/K]) was due mainly to oxygen deficiency and may be partially related to heat loss due to water evaporation. The convex shape of the plot at temperatures below 112 °C (>0.00260 [1/K]) suggests that microbial reactions were involved in raising the temperature of the biomass, discussed in the following section.

3.2. Validation of the model

After the heat source was estimated, the model needed to be validated. The temperature profiles of manure from the experiments and the model at different induction temperatures are shown in Fig. 2. Except for an induction temperature of 85 °C, the model successfully reproduced the experimental data and showed that temperature rise due to self-heating was initiated at 90 °C and 110 °C but not at 80 °C (Figs. 2a, 2c, and 2d). A discrepancy was found between the experimental and model data at the induction temperature of 85 °C (Fig. 2b); self-heating was observed in the experimental data but not in the model. At an induction temperature of 110 °C, the model reproduced a typical temperature profile, showing a 24-hour stagnation near 160 °C due to drying, but the fitting accuracy was low at temperatures above 170 °C.

Overall, the model developed could reproduce the self-heating of the torrefaction process.

Reproduction of the temperature stagnation corresponding to the drying period indicates that using the term “drying” is reasonable. In contrast, the model does not match the experimental data toward the end of the process (>170 °C). This was predictable because the model does not consider the heat balance associated with biomass decomposition. This decomposition includes both oxidation (exothermic) and pyrolysis (endothermic), and cannot be ignored at higher temperatures because of the temperature dependency of the reactions. A more complex model that considers the formation enthalpy of each species and the change in mass would be useful to increase fitting accuracy after the drying period (Kung and Ghoniem, 2019), although the present study was not designed to accomplish this.

The inaccurate predictions at the induction temperature of 85 °C may be due to underestimation of the heat source, resulting from (1) inaccurate estimation of Arrhenius parameters (activation energy and pre-exponential term) and (2) neglect of heat generation by microbial reactions. The latter is more plausible. As shown in Fig. 1b, the linearity of the Arrhenius plot was very good and the experimental and model data from the 110 to 160 °C temperature increase were in good agreement (Figs. 2c and 2d). This indicates that the estimates of the Arrhenius parameters were sufficiently accurate. In contrast, the Arrhenius plot loses linearity near <112 °C (Fig. 1a), strongly suggesting the existence of heat generation other than chemical oxidation. Thus, the heat source term may need to be modified to take this into account.

Adding a term to the heat source for microbial activity should improve the accuracy of the model. Kinetic models of microbial activity corresponding to microbial heat

248 generation have been proposed, such as zero-order, first-order, logistic, and monotypic
249 models, using the specific growth rate (Sheng and Yao, 2022). However, the present study
250 did not incorporate that modification due to the suspected presence of microbes active
251 within a higher temperature range than previously known. In general, the maximum
252 oxygen consumption rate and heat generation rate during composting are observed near
253 the mesophilic (43 °C) and thermophilic (*ca*. 60 °C) temperatures (Iwabuchi and Kimura,
254 1994). Furthermore, observations of the specific growth rate and oxygen consumption
255 rate of microbes indicate that mesophilic and thermophilic bacteria are most active at
256 43 °C and 54 °C, respectively, and some activity by thermotolerant bacteria is observed
257 within a temperature range of 68–74 °C (Miyatake and Iwabuchi, 2006). However, the
258 temperature profiles and Arrhenius plots in the present study suggested that microbial
259 activity was present, even at an extremely high temperature. Given that conventional
260 models describing microbial activity are parameterized to represent general behavior,
261 adding them into the model was not appropriate. The model is expected to be improved
262 further by verifying the existence of microbes active above 80 °C and determining the
263 heat source due to microbial action.
264
265 *3.3. Conditions for inducing self-heating of manure*
266 Figure 3 shows ambient pressures and ventilation rates under which self-heating is
267 induced. Self-heating was defined as the condition under which a temperature increase of
268 10 °C or more occurred within 24 hours. The mathematical model showed that the greater
269 the ambient pressure and the lower the ventilation rate at any given pressure, the lower
270 the temperature at which self-heating was induced. The lowest and highest induction
271 temperatures were 71 °C and 127 °C, respectively. At ventilation rates of 0.1 L min^{-1} kg-

AFS^{-1} or lower, no remarkable decrease in the induction temperature occurred after increasing the pressure, while at ventilation rates of 0.5 L min^{-1} kg-AFS^{-1} or greater, induction temperatures changed by more than 20 °C. The model also revealed that self-heating occurred even at ventilation rates of 0.05 L min^{-1} kg-AFS^{-1} or lower, but the rate of temperature increase was very slow.

The results demonstrated that both ambient pressure and ventilation rate are involved in the heat balance of the biomass. In addition, the relation between ambient pressure and inducing temperature was similar to the trend observed in a previous experimental study (Itoh et al., 2020), supporting the reliability of the model. Elevated pressure plays the role of reducing heat loss due to the latent heat of moisture evaporation. Evaporation is a physical phenomenon driven by the difference between the supposed saturated humidity of the biomass surface and the specific humidity of the gas (eq. [5]). The area of saturated humidity decreases as the ambient pressure increases at a given temperature (eq. [6]), indicating greater suppression of the driving force for evaporation at higher ambient pressures. In addition, the high-pressure environment may promote chemical oxidation reactions. Since the amount of dissolved oxygen in the water on biomass surface follows Henry's law, the higher the pressure, the more chemical oxidation is promoted. Lower ventilation rates resulted in less heat loss because the temperature of the feed gas was lower than the biomass temperature, and more heat is transferred from the biomass to the gas at higher ventilation rates (eq. [1]). Therefore, to minimize heat loss due to ventilation, the ventilation rate should be set as low as possible, or no ventilation should be used. However, ventilation also supplies the oxygen necessary for oxidation reactions, and an extremely low ventilation rate will increase the time required for the overall process.

The results also suggest the feasibility of a new torrefaction system that combines microbial and chemical reactions (Fig. S1). A previous study confirmed that dairy cattle manure should be heated to at least 85 °C to reliably induce self-heating (Itoh et al., 2019). However, the model also reveals that setting the ventilation rate lower than 0.1 L min^{-1} kg-AFS^{-1} induces self-heating of manure from 71 °C, a temperature achieved by microbial activity during the composting process. Thus, under appropriate ventilation and pressure conditions, self-heating of biomass up to the torrefaction temperature range can be induced from room temperature by a combination of microbial and chemical reactions. Demonstrating this has been attempted, but the transition to chemical reactions often fails, and inducing self-heating from room temperature to self-ignition of biomass with a high degree of reproducibility has not been successful. If the reaction mechanism can be elucidated from experimental and theoretical approaches and this system can be established in the future, carbonization of livestock manure will become more widespread.

3.4. Effects of ventilation and ambient pressure on the process

To investigate the effect of ventilation rate on the self-heating process, temperature profiles at different ventilation rates from both experiments and model are shown in Fig. 4. Note that the temperature profiles are shown only up to 200 °C because the model could not reproduce the process after the end of drying. In addition, at 2.2 L min^{-1} kg-AFS^{-1} only the experimental data are shown, as the model did not show a temperature increase under this condition. The experimental data indicated that the greater the ventilation rate, the shorter the time required for drying. The temperature profile for the beginning and drying periods differed significantly between each run at ventilation rates

of 1.8 and 2.2 L min^{-1} kg-AFS^{-1}. Moreover, approximately 40%wb moisture remained in the samples at the end of the experiment (60%wb initially) at 2.2 L min^{-1} kg-AFS^{-1}, even though the temperature increased above the boiling point of 180 °C at 1.0 MPa. The model fit well at 1.0 L min^{-1} kg-AFS^{-1}, but did not represent the experimental data well at 1.8 L min^{-1} kg-AFS^{-1} because of the pronounced effect of heat loss due to ventilation in the early stages of the process. This may have been caused by the model assumption that the temperatures of the exhaust gas and biomass are equal. In reality, the higher the ventilation rate, the shorter the contact time between the gas and the biomass, *i.e.*, the smaller the heat exchange, so the temperature of the exhaust gas is lower than the biomass temperature. Therefore, the effect of heat loss due to ventilation was inferred to be smaller in the experiment than in the model, leading to a smooth temperature increase from the initial stage. An increase in pressure resulted in temperature stagnation corresponding to drying to occur at higher temperatures, while the pressure barely affected the drying duration time (Fig. 5).

Results revealed that ventilation rate greatly affects the process time; greater ventilation rates can shorten the drying period but require more time to increase temperature at the beginning of the process. For practical operation, reducing the time required for the process is important for improving production efficiency. Thus, the ventilation rate should be set to a relatively low value (0.1–1.0 L min^{-1} kg-AFS^{-1}) until the drying period and then increased to 1.8 L min^{-1} kg-AFS^{-1} once the drying period begins.

The use of extremely low ventilation rates (<0.1 L min^{-1} kg-AFS^{-1}) effectively reduces heat losses due to ventilation, especially early in the process, but may also delay

344 temperature rise due to oxygen deficiency. During the drying period, greater ventilation
345 is recommended to shorten the drying period, but incurs the risk of incomplete drying if
346 the ventilation rate is too high (*e.g.*, 2.2 L min^{-1} kg-AFS^{-1}) because temperature and
347 moisture gradients in the reactor increase with ventilation rate. The risk also exists that
348 greater ventilation rates will accelerate oxidative decomposition of the biomass, resulting
349 in lower production efficiency, such as lower product yield and quality. Several studies
350 reported oxidative torrefaction had adverse effects on the process (Chen et al., 2014,
351 2013; Lu et al., 2012).
352
353 *3.5. Future studies*
354 Further research is needed, such as gaining an understanding of the size of the torrefaction
355 reactor in which self-heating occurs stably, to implement the self-heating torrefaction
356 system. Currently, experiments are being conducted in an adiabatic environment using an
357 oven to induce self-heating on a laboratory scale. However, in practical applications, no
358 such adiabatic environment will exist, and heat dissipation driven by the temperature
359 difference between the inside and outside of the reactor will occur. Due to the law of
360 surface-area-to-volume ratio, scaling up the reactor size will be effective to reduce heat
361 dissipation from the system, but the zero-dimensional model developed cannot answer
362 this question. Extension to 2- or 3-dimensional models that can account for heat transfer
363 is required in future studies.
364
365 **4. Conclusions**
366 A model was developed to predict the initial conditions that induce self-heating of manure
367 (60%wb) and to understand the effects of operating variables on temperature rise to the

end of drying. In the range of 0.05–3.0 L min^{-1} kg-AFS^{-1} of ventilation rate and 0.2–2.0 MPa of ambient pressure, the greater the ambient pressure and the lower the ventilation rate at any given pressure, the lower the temperature at which self-heating was induced. Self-heating of manure due to chemical oxidation also was revealed theoretically to be initiated at 71 °C. For the drying process, the model was not reliable at a 1.8 L min^{-1} kg-AFS^{-1} or higher ventilation rate. To shorten the process, the ventilation rate can be relatively low until the drying period when it can be increased moderately once the drying period begins.

Acknowledgements

This study was supported by Tanigurogumi Corporation, Japan.

References

Amon, B., Kryvoruchko, V., Amon, T., Zechmeister-Boltenstern, S., 2006. Methane, nitrous oxide and ammonia emissions during storage and after application of dairy cattle slurry and influence of slurry treatment. Agric Ecosyst Environ 112, 153–162. https://doi.org/10.1016/j.agee.2005.08.030

Basso, B., Ritchie, J.T., 2005. Impact of compost, manure and inorganic fertilizer on nitrate leaching and yield for a 6-year maize–alfalfa rotation in Michigan. Agric Ecosyst Environ 108, 329–341. https://doi.org/10.1016/j.agee.2005.01.011

Chen, W.-H., Lin, B.-J., Lin, Y.-Y., Chu, Y.-S., Ubando, A.T., Show, P.L., Ong, H.C., Chang, J.-S., Ho, S.-H., Culaba, A.B., Pétrissans, A., Pétrissans, M., 2021. Progress in biomass torrefaction: Principles, applications and challenges. Prog Energy Combust Sci 82, 100887. https://doi.org/10.1016/j.pecs.2020.100887

Chen, W.-H., Lu, K.-M., Lee, W.-J., Liu, S.-H., Lin, T.-C., 2014. Non-oxidative and oxidative torrefaction characterization and SEM observations of fibrous and ligneous biomass. Appl Energy 114, 104–113. https://doi.org/10.1016/j.apenergy.2013.09.045

Chen, W.-H., Lu, K.-M., Liu, S.-H., Tsai, C.-M., Lee, W.-J., Lin, T.-C., 2013. Biomass torrefaction characteristics in inert and oxidative atmospheres at various superficial velocities. Bioresour Technol 146, 152–160. https://doi.org/10.1016/j.biortech.2013.07.064

Daouk, E., van de Steene, L., Paviet, F., Martin, E., Valette, J., Salvador, S., 2017.

Oxidative pyrolysis of wood chips and of wood pellets in a downdraft continuous fixed bed reactor. Fuel 196, 408–418. https://doi.org/10.1016/j.fuel.2017.02.012

Dupont, C., Chiriac, R., Gauthier, G., Toche, F., 2014. Heat capacity measurements of various biomass types and pyrolysis residues. Fuel 115, 644–651. https://doi.org/10.1016/j.fuel.2013.07.086

Fernandez-Lopez, M., Pedrosa-Castro, G.J., Valverde, J.L., Sanchez-Silva, L., 2016. Kinetic analysis of manure pyrolysis and combustion processes. Waste Management 58, 230–240. https://doi.org/10.1016/j.wasman.2016.08.027

He, C., Tang, C., Li, C., Yuan, J., Tran, K.-Q., Bach, Q.-V., Qiu, R., Yang, Y., 2018. Wet torrefaction of biomass for high quality solid fuel production: A review. Renewable and Sustainable Energy Reviews 91, 259–271. https://doi.org/10.1016/j.rser.2018.03.097

Itoh, T., Iwabuchi, K., Maemoku, N., Chen, S., Taniguro, K., 2020. Role of ambient pressure in self-heating torrefaction of dairy cattle manure. PLoS One 15, e0233027. https://doi.org/10.1371/journal.pone.0233027

Itoh, T., Iwabuchi, K., Maemoku, N., Sasaki, I., Taniguro, K., 2019. A new torrefaction system employing spontaneous self-heating of livestock manure under elevated pressure. Waste Management 85, 66–72. https://doi.org/10.1016/j.wasman.2018.12.018

Iwabuchi, K., Kimura, T., 1994. Aerobic Biodegradation of Dairy Cattle Feces (Part 1) Heat Production Rate and Oxygen Uptake Rate. Journal of the Japanese Society of Agricultural Machinery 56, 67–74. https://doi.org/10.11357/jsam1937.56.2_67

Iwabuchi, K., Kimura, T., Otten, L., 1999. Effect of volumetric water content on thermal properties of dairy cattle feces mixed with sawdust. Bioresour Technol 70, 293–297. https://doi.org/10.1016/S0960-8524(99)00038-3

Kung, K.S., Ghoniem, A.F., 2019. A decentralized biomass torrefaction reactor concept. Part II: Mathematical model and scaling law. Biomass Bioenergy 125, 204–211. https://doi.org/10.1016/j.biombioe.2018.12.001

Li, D.-C., Jiang, H., 2017. The thermochemical conversion of non-lignocellulosic biomass to form biochar: A review on characterizations and mechanism elucidation. Bioresour Technol 246, 57–68. https://doi.org/10.1016/j.biortech.2017.07.029

López-González, D., Parascanu, M.M., Fernandez-Lopez, M., Puig-Gamero, M., Soreanu, G., Avalos-Ramírez, A., Valverde, J.L., Sanchez-Silva, L., 2017. Effect of different concentrations of O2 under inert and CO2 atmospheres on the swine manure combustion process. Fuel 195, 23–32. https://doi.org/10.1016/j.fuel.2017.01.041

Lu, K.-M., Lee, W.-J., Chen, W.-H., Liu, S.-H., Lin, T.-C., 2012. Torrefaction and low temperature carbonization of oil palm fiber and eucalyptus in nitrogen and air atmospheres. Bioresour Technol 123, 98–105. https://doi.org/10.1016/j.biortech.2012.07.096

Maeda, M., Zhao, B., Ozaki, Y., Yoneyama, T., 2003. Nitrate leaching in an Andisol treated with different types of fertilizers. Environmental Pollution 121, 477–487. https://doi.org/10.1016/S0269-7491(02)00233-6

Milhé, M., van de Steene, L., Haube, M., Commandré, J.-M., Fassinou, W.-F., Flamant, G., 2013. Autothermal and allothermal pyrolysis in a continuous

fixed bed reactor. J Anal Appl Pyrolysis 103, 102–111. https://doi.org/10.1016/j.jaap.2013.03.011

Miyatake, F., Iwabuchi, K., 2006. Effect of compost temperature on oxygen uptake rate, specific growth rate and enzymatic activity of microorganisms in dairy cattle manure. Bioresour Technol 97, 961–965. https://doi.org/10.1016/j.biortech.2005.04.035

Muhammad, J., Khan, S., Su, J.Q., Hesham, A.E.-L., Ditta, A., Nawab, J., Ali, A., 2020. Antibiotics in poultry manure and their associated health issues: a systematic review. J Soils Sediments 20, 486–497. https://doi.org/10.1007/s11368-019-02360-0

Pham, X.-H., Piriou, B., Salvador, S., Valette, J., van de Steene, L., 2018. Oxidative pyrolysis of pine wood, wheat straw and miscanthus pellets in a fixed bed. Fuel Processing Technology 178, 226–235. https://doi.org/10.1016/j.fuproc.2018.05.029

Rizzo, A.M., Pettorali, M., Nistri, R., Chiaramonti, D., 2019. Mass and energy balances of an autothermal pilot carbonization unit. Biomass Bioenergy 120, 144–155. https://doi.org/10.1016/j.biombioe.2018.11.009

Sheng, C., Yao, C., 2022. Review on Self-Heating of Biomass Materials: Understanding and Description. Energy & Fuels 36, 731–761. https://doi.org/10.1021/acs.energyfuels.1c03369

Spielmeyer, A., 2018. Occurrence and fate of antibiotics in manure during manure treatments: A short review. Sustain Chem Pharm 9, 76–86. https://doi.org/10.1016/j.scp.2018.06.004

Toei, R., Okazaki, M., Tamon, H., 1994. Conventional basic design for convection or conduction dryers. Drying Technology 12, 59–97. https://doi.org/10.1080/07373939408959950

Tojo, S., Watanabe, K., Ai, B., Chao, A.C., 1994. Drying Characteristics of Cattle Excrement and Food Processing Residues. Journal of the Japanese Society of Agricultural Machinery 56, 57–64. https://doi.org/10.11357/jsam1937.56.5_57

Wagner, W., Pruss, A., 1993. International Equations for the Saturation Properties of Ordinary Water Substance. Revised According to the International Temperature Scale of 1990. Addendum to J. Phys. Chem. Ref. Data 16, 893 (1987). J Phys Chem Ref Data 22, 783–787. https://doi.org/10.1063/1.555926

Walling, E., Trémier, A., Vaneeckhaute, C., 2020. A review of mathematical models for composting. Waste Management 113, 379–394. https://doi.org/10.1016/j.wasman.2020.06.018

Wang, T., Zhai, Y., Zhu, Y., Li, C., Zeng, G., 2018. A review of the hydrothermal carbonization of biomass waste for hydrochar formation: Process conditions, fundamentals, and physicochemical properties. Renewable and Sustainable Energy Reviews 90, 223–247. https://doi.org/10.1016/j.rser.2018.03.071

Wirth, B., Mumme, J., 2014. Anaerobic Digestion of Waste Water from Hydrothermal Carbonization of Corn Silage. Applied Bioenergy 1, 1–10. https://doi.org/10.2478/apbi-2013-0001

Wirth, B., Reza, M.T., 2016. Continuous Anaerobic Degradation of Liquid Condensate from Steam-Derived Hydrothermal Carbonization of Sewage Sludge. ACS Sustain Chem Eng 4, 1673–1678. https://doi.org/10.1021/acssuschemeng.5b01607

499

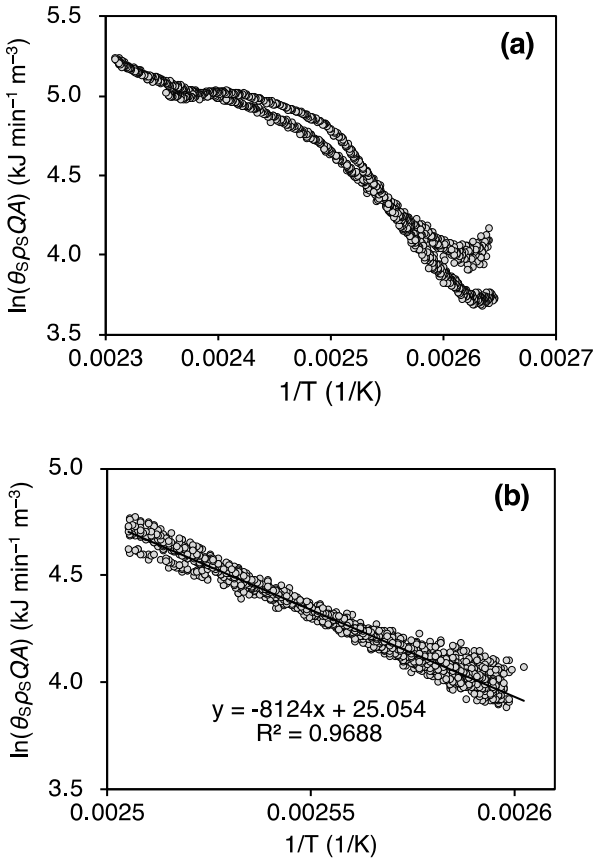

500

501 Fig. 1. Arrhenius plots at (a) 105–160 °C and (b) 112–126 °C under conditions of 0.83 L

502 min^{-1} kg-AFS^{-1} and 1.0 MPa.

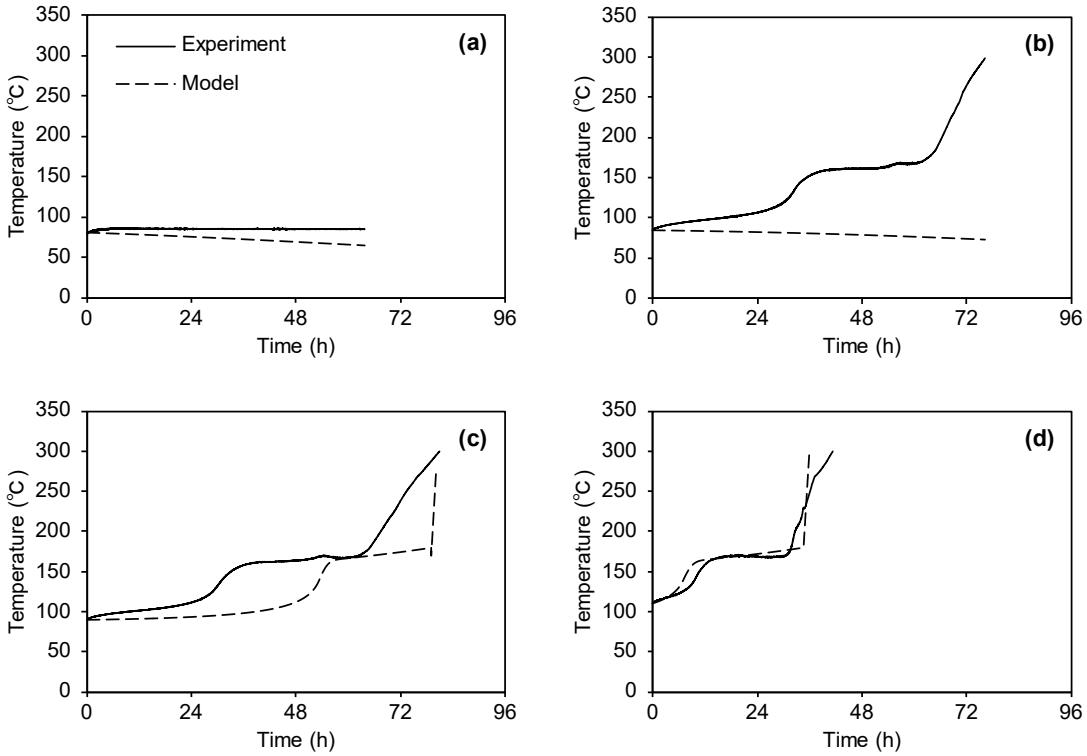

503

504 Fig. 2. Experimental and model temperature profiles at induction temperatures of (a)

505 80 °C, (b) 85 °C, (c) 90 °C, and (d) 110 °C using a ventilation rate of 0.8 L min^{-1} kg-

506 AFS^{-1} and ambient pressure of 1.0 MPa.

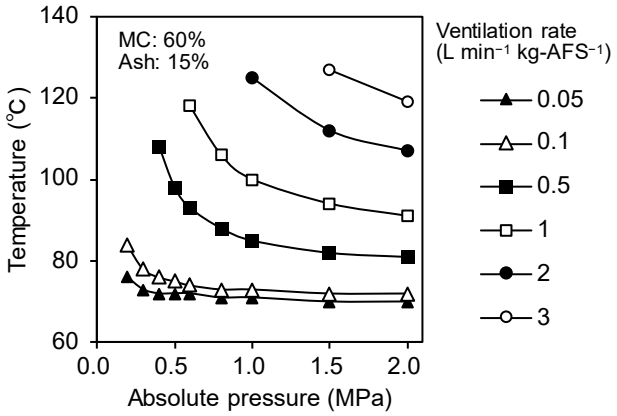

507

508 Fig. 3. Initial conditions that induce self-heating of dairy manure.

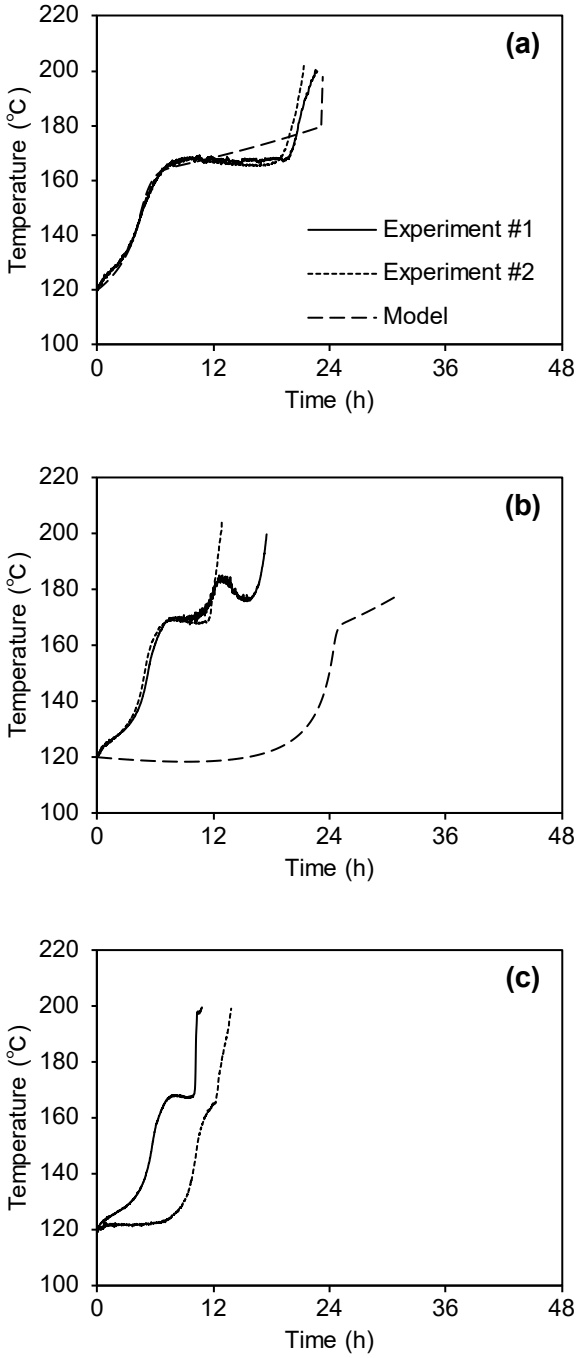

509

510 Fig. 4. Effects of ventilation rate on temperature rise during the process: (a) 1.0 L min^{-1}

511 kg-AFS^{-1}, (b) 1.8 L min^{-1} kg-AFS^{-1}, and (c) 2.2 L min^{-1} kg-AFS^{-1}.

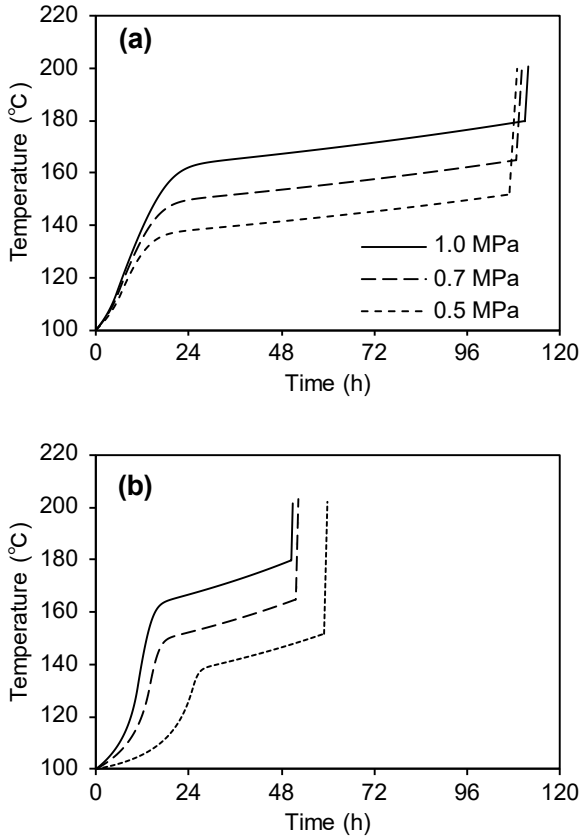

512

513 Fig. 5. Effects of ambient pressure on temperature rise during the process: (a) 0.2 L

514 min^{-1} kg-AFS^{-1} and (b) 0.5 L min^{-1} kg-AFS^{-1}.